The Calcium Current of *Helix* Neuron

NORIO AKAIKE, KAI S. LEE, and ARTHUR M. BROWN

From the Department of Physiology and Biophysics, University of Texas Medical Branch, Galveston, Texas 77550

ABSTRACT Calcium current, I_{Ca}, was studied in isolated nerve cell bodies of *Helix aspersa* after suppression of Na^+ and K^+ currents. The suction pipette method described in the preceding paper was used. I_{Ca} rises to a peak value and then subsides exponentially and has a null potential of 150 mV or more and a relationship with $[Ca^{2+}]_o$ that is hyperbolic over a small range of $[Ca^{2+}]_o$'s. When $[Ca^{2+}]_i$ is increased, I_{Ca} is reduced disproportionately, but the effect is not hyperbolic. I_{Ca} is blocked by extracellular Ni^{2+}, La^{3+}, Cd^{2+}, and Co^{2+} and is greater when Ba^{2+} and Sr^{2+} carry the current. Saturation and blockage are described by a Langmuir adsorption relationship similar to that found in *Balanus*. Thus, the calcium conductance probably contains a site which binds the ions referred to. The site also appears to be voltage-dependent. Activation and inactivation of I_{Ca} are described by first order kinetics, and there is evidence that the processes are coupled. For example, inactivation is delayed slightly in its onset and τ inactivation depends upon the method of study. However, the currents are described equally well by either a noncoupled Hodgkin-Huxley *mh* scheme or a coupled reaction. Facilitation of I_{Ca} by prepulses was not observed. For times up to 50 ms, currents even at small depolarizations were accounted for by suitable adjustment of the activation and inactivation rate constants.

INTRODUCTION

Calcium currents are involved in a variety of functions including neural signalling, excitation-contraction and excitation-secretion coupling, and ciliary reversal (Fatt and Katz, 1953; Hagiwara and Naka, 1964; Katz and Miledi, 1967; Baker et al., 1971; Kostyuk et al., 1974*a*, *b*; Standen, 1975; Hagiwara, 1975). I_{Ca} has distinctive pharmacological characteristics in barnacle muscle (Hagiwara, 1975), but, in many tissues its voltage dependence, kinetics, and ionic selectivity are not known with great certainty. The purpose of the present experiments was to characterize I_{Ca} with respect to these properties using the suction pipette method described in the preceding paper (Lee et al.). Two reports published after this paper was submitted have examined some of these properties (Hencek and Zachar, 1977; Kostyuk et al., 1977). We found that I_{Ca} has single activation and single inactivation components that may be coupled and can be encompassed by a single set of kinetics. The Ca^{2+} conductance, G_{Ca}, transports Ca^{2+} and other divalent cations but not Na^+, and has a binding site for divalent cations similar to that proposed by Hagiwara (1975).

METHODS

The suction pipette voltage clamp and internal perfusion system was described in the

preceding paper (Lee et al.). The shunt resistance was very large in most of the experiments so that compensation of voltage clamp currents was not required. In some experiments current and voltage records were digitized every 5 μs using a digital oscilloscope having 9 bit resolution (model 1090, Nicolet Instrument Corp., Madison, Wisc.) and stored on a digital tape recorder (Kennedy model 9700 C. J. Kennedy Co., Altadena, Calif.). At steps from the usual holding potentials to voltages $< +100$ mV, the capacitative current transient and leakage current associated with the separated I_{Ca} could be subtracted by a computer (PDP 11/40, Digital Equipment Corp., Marlboro, Mass.) using values obtained from equivalent hyperpolarizing voltage steps. At voltages $> +100$ mV, the leakage current rectifies in the outward direction (Fig. 8; Lee et al.), and this was corrected for by using average values similar to those shown in the referenced figure. Activation time constants, τ_m's, were determined from semilogarithmic plots of the time-to-peak current after peeling off the amount of inactivation at these times by simple backwards extrapolation. τ_m's were also calculated from semilogarithmic plots of the tail currents elicited by second voltage steps to different values at the peak of the transient current evoked by a conditioning step. Inactivation time constants were calculated from the time-course of inactivation during single voltage steps and from the effects of conditioning voltage prepulses of varying duration and amplitude on the peak current elicited by a test voltage step. Steady-state activation and inactivation values were determined using test voltage steps and for inactivation, conditioning prepulses between 30 and 200 ms in duration with variable amplitudes.

Effects of divalent ions were tested either by substitution for Ca^{2+} in normal snail Ringer or in zero Mg^{2+} snail Ringer. The compositions are shown in Table I. The organic calcium current blocker Verapamil (Knoll) was used in a dose of 3×10^{-5} M.

Calcium liquid ion exchanger electrodes were kindly prepared for us by Dr. Normand Hebert and were used to measure the calcium activity of many of our solutions. The electrodes had selectivities over Mg^{2+} and K^+ of 3×10^4 and 10^5, respectively, and had slopes of 29 mV per 10-fold change of $[Ca^{2+}]$ over the range of 10^{-5}–10^{-3} M and 20 mV per 10-fold change $[Ca^{2+}]$ over the range of 10^{-5}–10^{-7} M.

RESULTS

A total of >150 *Helix aspersa* neurons was examined in the present experiments, and the results of each aspect of the investigation were checked in at least five neurons. Inasmuch as the time-courses of the calcium and potassium currents overlap, they could interfere with each other. Therefore, further blockage of the Cs^+-suppressed clamp currents was attempted by using extracellular TEA or intracellular TEA or tetramethyl-ammonium ions. No additional effects were observed.

Substitution of either aspartate$^-$, isethionate$^-$, or methanesulfonate$^-$ for Cl^- in the extracellular fluid also did not affect the inward currents. After blockage of K^+ currents with Cs^+ and Na^+ current with substitution of $Tris^+$ for Na^+ or substitution of sucrose or glucose for NaCl, the voltage clamp currents shown in Fig. 1A remained. A slowly rising inward current due to Ca^{2+} appeared at depolarizing voltage steps of 5–10 mV from the holding potential of −60 mV, rose smoothly, reached its peak within 5–10 ms, and persisted over the subsequent 15–100 ms. We have not observed an inflection on the rising phase as reported by Magura (1977). A small component of inward current continued for several seconds in most experiments. The onset of the current was obscured by the capacitative current transient, and the first 500 μs were not resolved. A

transient peak occurring at 1–3 ms appeared at larger depolarizing voltages, declined, and merged with the slowly inactivating current. The peak was reached more quickly, became smaller, flattened, and eventually was nullified as the voltage steps were made increasingly positive. An outward peak was usually not detectable at high voltages, and the positive potential at which zero current first occurred is termed the null potential. The fall of current was exponential and could be fitted by a single time constant which was voltage-dependent (Fig. 1 C).

TABLE I

IONIC COMPOSITION OF SNAIL RINGER SOLUTIONS

Solution	NaCl	Tris Cl	KCl	CsCl	Cs aspartate	K aspartate	$CaCl_2$	$MgCl_2$	Glucose
					mM				
External solution									
Normal	85	5	5	–	–	–	10	15	5.5
Na, K-free Tris, Cs	–	90	–	5	–	–	10	15	5.5
K, Ca-free Cs, Co	85	5	–	5	–	–	Co 10	15	5.5
Na, K, Ca-free Tris, Cs, Co	–	85	–	5	–	–	Co 10	15	5.5
Na, K-free 2 mM Ca	–	95	–	5	–	–	2	15	–
Na, K-free 10 mM Ca	–	80	–	5	–	–	10	15	–
Na, K-free 40 mM Ca	–	35	–	5	–	–	40	15	–
Na, K, Mg-free 2 mM Ca	–	131	–	5	–	–	2	–	5.5
Na, K, Mg-free 10 mM Ca	–	115	–	5	–	–	10	–	5.5
Na, K, Mg-free 40 mM Ca	–	55	–	5	–	–	40	–	5.5
Internal solution									
Normal	–	–	–	–	–	135	–	–	–
CsCl	–	–	–	135	–	–	–	–	–
Cs aspartate	–	–	–	–	135	–	–	–	–

The voltage relationships of the peak currents after leakage correction are shown in Fig. 1 D. In 10% of the cells the transient current clearly reversed its direction at large depolarizations (Fig. 2). The ascending limb of the transient *I-V* relationship was steeper in these cells, and the reversal potential of the transient current was less positive than the more usual null potential.

The inward current, separated in the manner we have described, and its *I-V* relationship were unaffected by TTX (5×10^{-6} M). Also, when the Na^+ current was blocked initially with TTX, Tris substitution for Na^+ actually enhanced inward current. As we shall demonstrate, the inward current, separated as we have described, was altered by changes in internal and external Ca^{2+} concentration, $[Ca^{2+}]_{i,o}$, blocked by certain divalent and trivalent cations and an organic

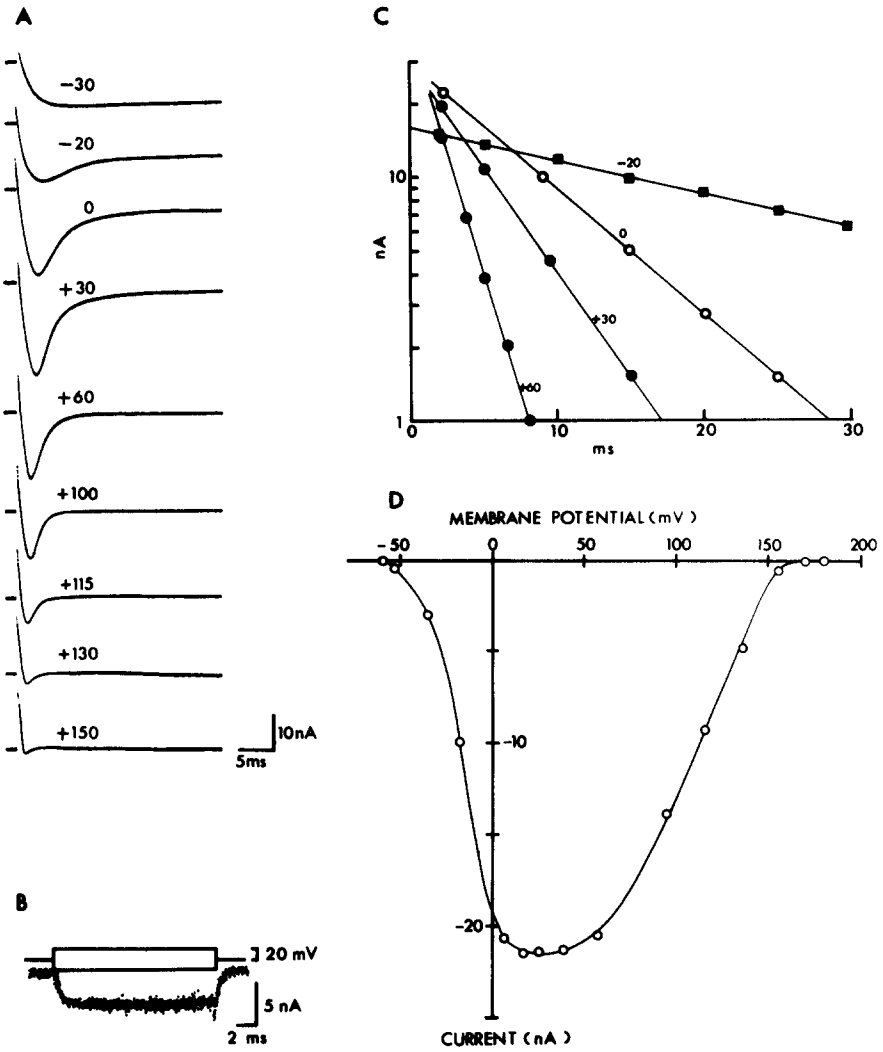

FIGURE 1. Customary calcium currents, I_{Ca}, in snail neurons after suppression of Na^+ and K^+ currents. (A) Ca^{2+} current records obtained under voltage clamp from a neuron in Na^+, K^+-free, Tris, Cs^+ solutions. The numbers are the command voltages (mV) applied from holding potential, V_H, of −60 mV. (B) I_{Ca} evoked by adding the currents elicited by equivalent hyperpolarizing and depolarizing steps of 20 mV from V_H of −60 mV. (C) Exponential fall in the currents shown in A. (D) I-V relationship for I_{Ca} obtained from records such as those in A. Abscissa: membraine potential (mV). Ordinate: peak inward current elicited by command pulse. A clear reversal current was not observed; rather the current approaches zero values at a null potential of 168 mV.

Ca^{2+} current blocker, and enhanced by Ba^{2+} and Sr^{2+}. It is therefore carried by Ca^{2+} and is referred to as I_{Ca}.

Effects of Changing $[Ca^{2+}]_i$ upon the Transient Current

Intracellular calcium activities were varied from 10^{-5} M to 1.2×10^{-8} M. The high values were measured in internal solutions of CsCl (Table I, Lee et al.) and the lowest values in the Cs aspartate solutions to which 1 mM EDTA was added. The measured calcium activity in the Cs aspartate solution was 2.0×10^{-6} M, which is in good agreement with the theoretical value predicted from the calcium aspartate stability constant of $10^{1.6}$ (Martell and Sillén, 1971) and the

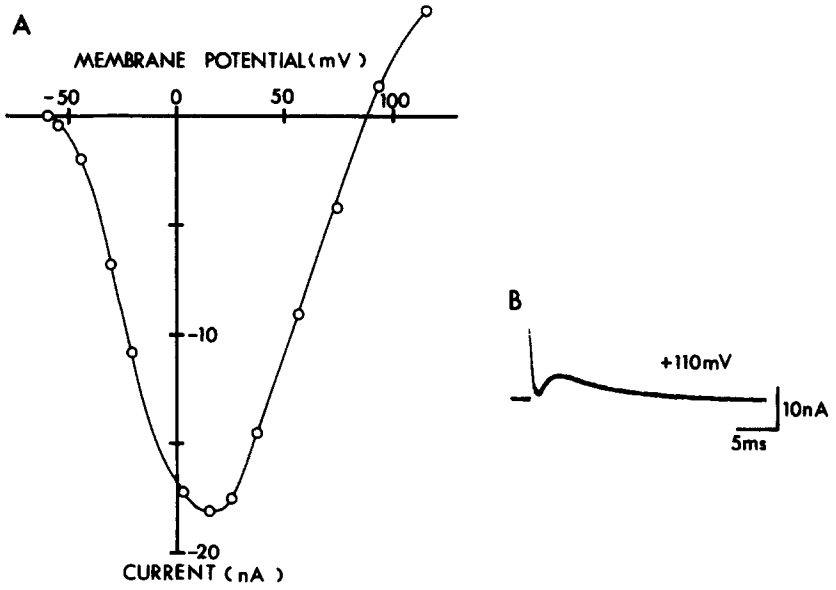

FIGURE 2. Examples of less common patterns of I_{Ca} in snail neurons. (A) Current-voltage relationship of peak transient currents. V_H: −60 mV. Note the clear current reversal at 88 mV. (B) In this neuron, I_{Ca} clearly reversed its inward direction at the large depolarizing step from V_H of −60 mV to +110 mV.

value of 10^{-5} M Ca^{2+} for the distilled water used to make our solutions.

The peak transient currents in 10 mM Ca_o^{2+} fell as $[Ca^{2+}]_i$ was increased at all voltages, and the *I-V* relationships for the various $[Ca^{2+}]_i$'s are shown in Fig. 3 A. The relationship between peak inward current at a given voltage and $[Ca^{2+}]_i$ is shown in Fig. 5 D and is neither hyperbolic nor exponential. The null potentials became less positive at higher Ca_i^{2+}'s and the changes in null potential had a Nernst-type relationship to the values of $[Ca^{2+}]_i$ (Fig. 3 B). As $[Ca^{2+}]_i$ was increased, the thresholds for inward current shifted in the hyperpolarizing direction, the downward limbs of the *I-V* curves became less steep, and the nadirs shifted to more depolarized potentials. The opposite sequence occurred when $[Ca^{2+}]_o$ was increased at constant $[Ca^{2+}]_i$ and this result is shown in Fig. 5 A.

Increasing $[Ca^{2+}]_i$ had substantial effects on input resistance (Fig. 4). These effects were concentration-and time-dependent. The transient current was not

affected as quickly as the input resistance but fell more precipitously. I_{Ca} measurements therefore had to be made with these constraints in mind.

Effects of Changing $[Ca^{2+}]_o$ upon the Transient Current

We tested the effects of increasing $[Ca^{2+}]_o$ within 3–5 min of the change because longer exposures reduced membrane resistance and inward currents. Effects due to lower $[Ca^{2+}]_o$ were examined between 5 and 10 min after the change in

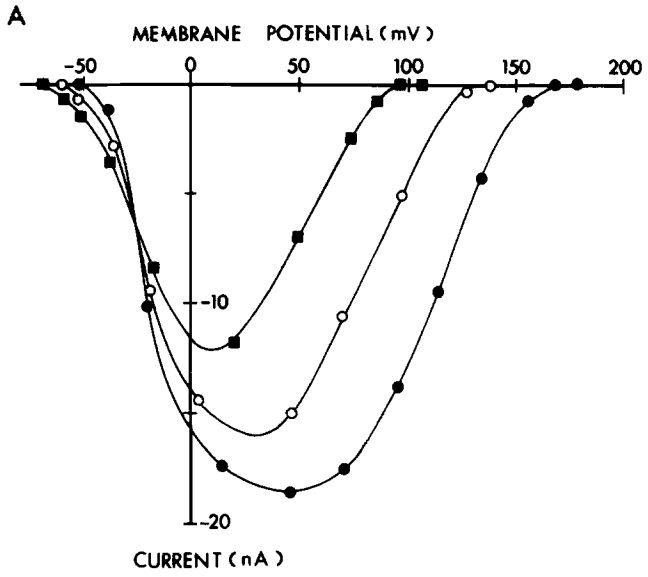

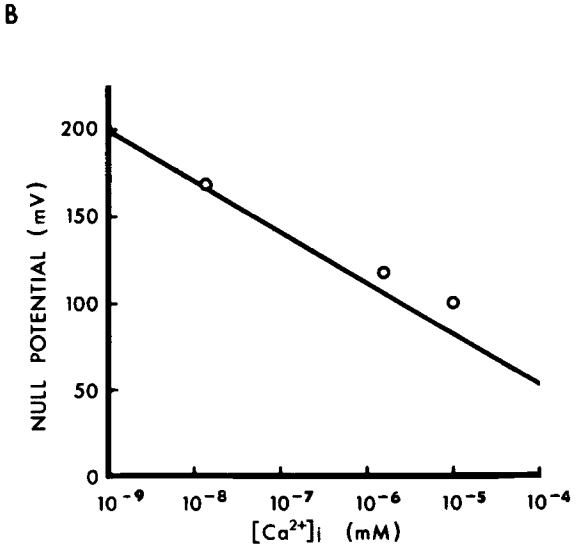

solution because of similar effects. Currents were increased in 40 mM Ca_o^{2+} and reduced but still present after 8 min in 2 mM Ca_o^{2+}. The null potentials became more positive with increases in $[Ca^{2+}]_o$ and less positive with reductions in $[Ca^{2+}]_o$. The effects of changes in $[Ca^{2+}]_o$ on threshold currents were not detectable in snail Ringer solution containing 15 mM Mg^{2+}, but the slopes of the ascending limbs of the *I-V* curves were steeper at higher $[Ca^{2+}]_o$'s. These aspects were examined further in zero Mg_o^{2+} solutions. The *I-V* relationships for the transient Ca^{2+} current in 2, 10, and 40 mM Ca_o^{2+} are shown in Fig. 5 A, and the effects of increasing $[Ca^{2+}]_o$ on thresholds, ascending limbs, and lowest points already referred to are observed. The measured Ca^{2+} activity of the internal perfusion solution was 1.6×10^{-6} M, and this value was used in calculations of E_{Ca}, the calcium equilibrium potential, in the various $[Ca^{2+}]_o$ solutions. The Ca^{2+} activity coefficient determined from the electrode measurements in the various extracellular solutions was 0.65. The null potentials and the E_{Ca}'s were similar as shown in Fig. 5 B.

The peak values of the transient current have a hyperbolic relationship with $[Ca^{2+}]_o$ at constant voltage steps. This is shown in Fig. 5 C where the voltage was stepped from V_H of −60 mV to +25 mV in the different $[Ca^{2+}]_o$ solutions. The results are the same with or without Mg_o^{2+}. A similar relationship between the maximum rate of rise of the barnacle muscle action potential and $[Ca^{2+}]_o$ was found by Hagiwara and Takahashi (1967) and by using their argument that the relationship is due to a calcium binding reaction we have

$$I_{Ca}(V) = \frac{I_{Ca\ max}(V)}{1 + K_{Ca}(V)/[Ca^{2+}]_o}, \quad (1)$$

where I_{Ca} is the peak transient current at a given voltage, V; $I_{Ca\ max}(V)$ is I_{Ca} when all the sites are occupied by Ca^{2+}; and $K_{Ca}(V)$ is the dissociation constant of the calcium binding site. The value for K_{Ca} was calculated using the data obtained from different $[Ca^{2+}]_o$ solutions at membrane potentials near 0 mV (Fig. 5 C) and was 5.4 mM. This value is about one-third that reported for the Ca^{2+} binding site in barnacle muscle (Hagiwara, 1975). A new finding is that the K_{Ca} values are increased at higher voltages. Thus at +50, +75, and +100 mV, they were 10.4, 26, and 82 mM, respectively.

FIGURE 3 (*Opposite*). Effects of changing $[Ca^{2+}]_i$ at constant $[Ca^{2+}]_o$ on I_{Ca}. (A) *I-V* relationship determined from step changes of membrane potential from V_H of −70 mV using internal solutions of (■) CsCl, (○) Cs aspartate, and (●) Cs aspartate plus 1 mM EDTA. Each current-voltage relation was plotted 15–20 min after changing the internal perfusate. Note the obvious effects on current thresholds, peak transient currents and null potentials. (B) Relationship between null potential $E_{Ca^{2+}}$ and $[Ca^{2+}]_i$. Data from same cell. A straight line was calculated by the equation

$$E_{Ca} = 29 \log \frac{f \cdot 10^{-2}}{[Ca^{2+}]_i},$$

where Ca^{2+} activity coefficient (f), determined using a Ca^{2+} liquid ion exchanger microelectrode is 0.65, and $[Ca^{2+}]_i$ was measured directly.

Effects of Divalent and Trivalent Cations and Verapamil upon I_{Ca}

Equimolar substitution of Ba^{2+} for Ca^{2+} increased the transient current and made the null potential more positive (Fig. 6 A). Sr^{2+} had similar effects so that the order was $Ba^{2+} = Sr^{2+} > Ca^{2+}$. Co^{2+} decreased the transient Ca^{2+}, Ba^{2+}, and Sr^{2+} currents to equivalent values (Fig. 6 B). There were no differences in threshold currents, and the shape of the *I-V* curves allowing for differences in

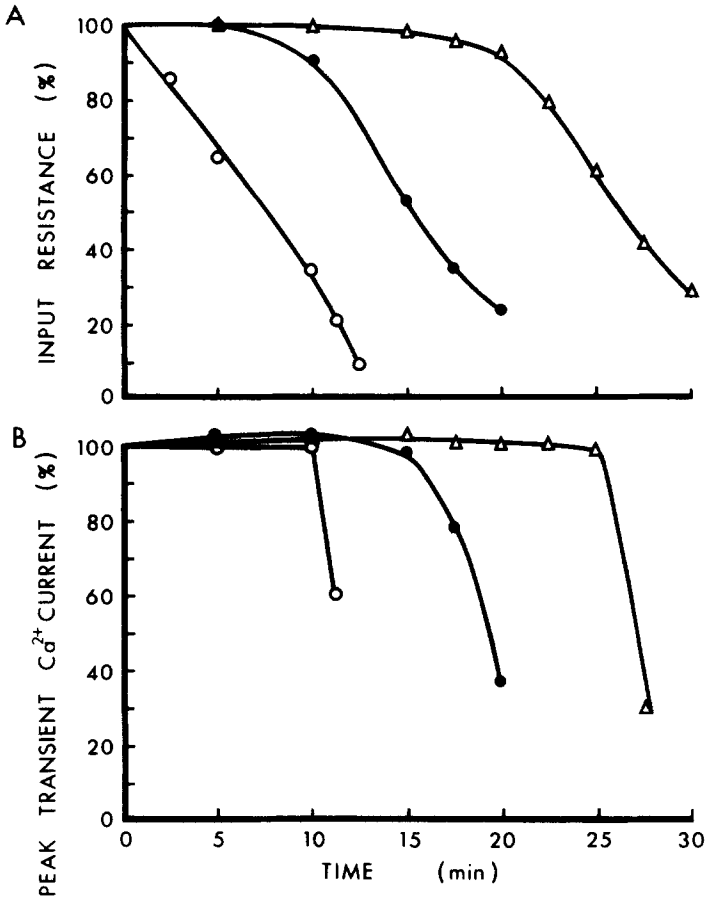

FIGURE 4. Time-courses of (A) input resistance and (B) Ca^{2+} currents in three different neurons perfused externally with constant $[Ca^{2+}]_o$ and internally with increased $[Ca^{2+}]_i$ (△) of 10^{-5}, (●) 3×10^{-5}, and (○) 10^{-4} M.

scale was similar although its nadir was shifted towards slightly lower voltages by Co^{2+}.

Ni^{2+} was the most effective blocker of the transient Ca^{2+} current and its blocking actions occurred at concentrations of 10^{-5} M (Fig. 7 A). The inhibitory effectiveness had the order $Ni^{2+} \gg La^{3+} \gg Cd^{2+} > Co^{2+} \gg Mg^{2+}$ in the presence of Ca^{2+}. La^{3+} at < 0.1 mM and Co^{2+} at < 1 mM temporarily enhanced the transient current. Concentrations of divalent ions between 1 and 10 mM also increased membrane resistance slightly. At the lowest concentrations the effects

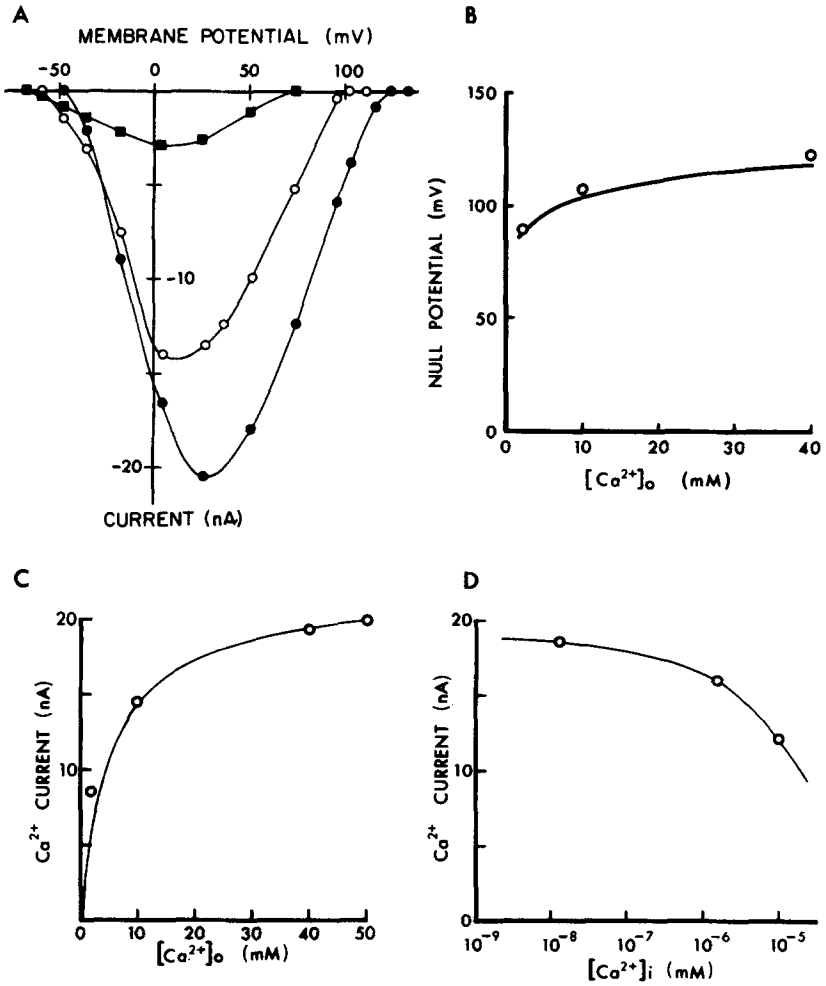

FIGURE 5. Effects of changes in $[Ca^{2+}]_o$ on I_{Ca} and a comparison with the effects of changes in $[Ca^{2+}]_i$. (A) Ca^{2+} currents in test solutions containing different $[Ca^{2+}]_o$ as a function of membrane potential obtained by voltage clamp of a neuron in Na^+, K^+, Mg^{2+}-free, $Tris^+$, Cs^+ solution. V_H: −70 mV. (■) 2 mM Ca^{2+}; (○) 10 mM Ca^{2+}; and (●) 40 mM Ca^{2+}. Note the effects on threshold, peak and null currents. (B) Relationship between null potential $E_{Ca^{2+}}$ and $[Ca^{2+}]_o$. A theoretical curve is calculated from

$$E_{Ca} = 29 \log \frac{f[Ca^{2+}]_o}{1.6 \times 10^{-6}},$$

where 1.6×10^{-6} is the measured Ca^{2+} activity in the Cs aspartate internal solution and Ca^{2+} activity coefficient (f) is 0.65. (C) The peak Ca^{2+} currents measured at 0 mV in the test solutions with different $[Ca^{2+}]_o$. The solid line is described by Eq. 1 in the text. (D) Relationship between peak I_{Ca} and $[Ca^{2+}]_i$. Relationship is not fitted by eq. 1 and the solid line is drawn through the points by eye.

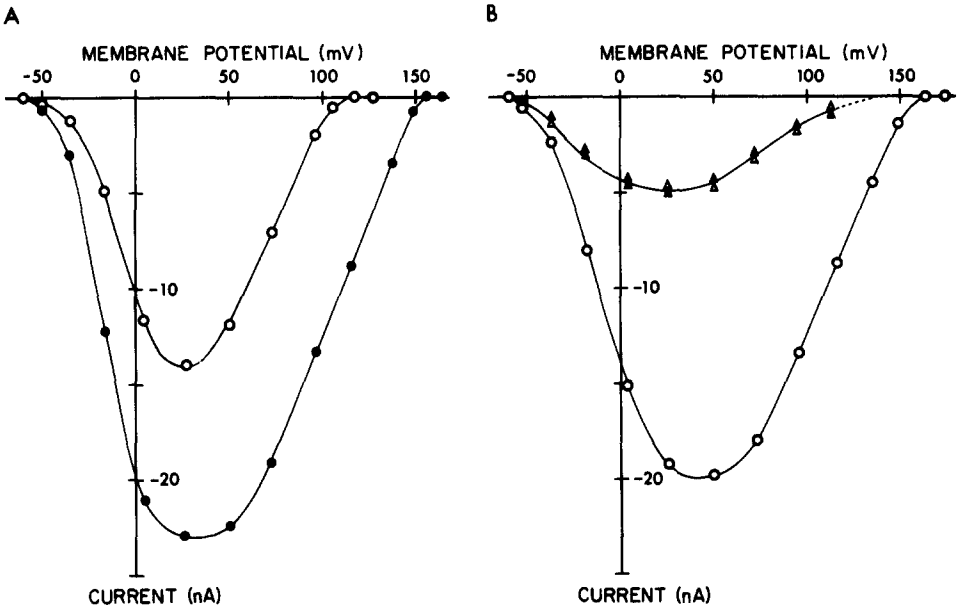

FIGURE 6. Actions of divalent cations on I_{Ca}. (A) Current-voltage relation at the peak of the inward currents during voltage clamp of a neuron in Na^+, K^+, Mg^{2+}-free $Tris^+$, Cs^+ Ringer solution containing 10 mM (○) Ca^{2+} or (●) Ba^{2+}. V_H: −60 mV. (B) Current-voltage relation in a neuron at 3 min after the application of test solution containing 10 mM (△) Ca^{2+} or (▲) Ba^{2+}. The test solutions contained 3 mM Co^{2+} and 12 mM Mg^{2+}. (○) Control in Na^+, K^+, Mg^{2+}-free $Tris^+$, Cs^+ Ringer solution with 10 mM Ca^{2+}. V_H: −60 mV.

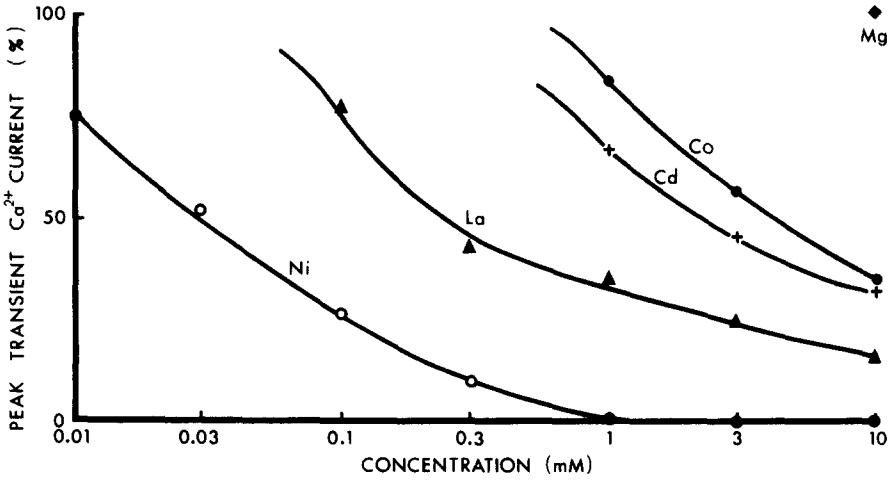

FIGURE 7. Blocking effects of divalent and trivalent cations on Ca^{2+} current. The relative inward currents are plotted against the concentration of blocking cations. Each test solution contained 10 mM Ca^{2+} and 15 mM Mg^{2+}. Recording was made 5 min after the application of each test solution. Lines drawn by eye.

were reversible but at higher concentration recovery was only partial.

The organic Ca^{2+} blocking drug, Verapamil, also inhibited the transient current. Blockage occurred over the entire voltage range and appeared to be most pronounced at the smallest and largest depolarizations (Fig. 8). The null potential also seemed to be less positive but the difference is uncertain because of the relatively large leakage currents at large depolarizing potentials.

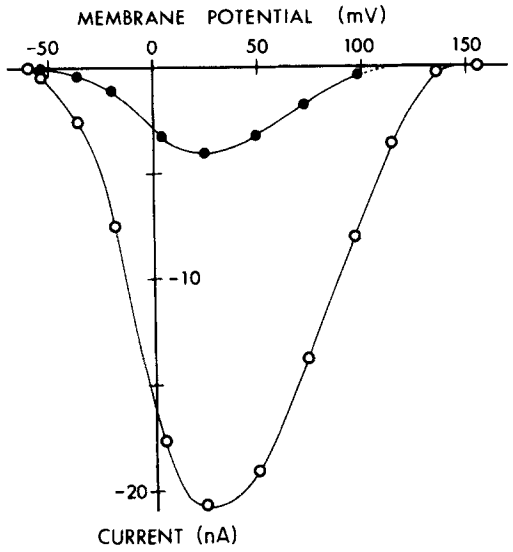

FIGURE 8. Effect of an organic Ca^{2+} antagonist, Verapamil, on the inward current associated with step changes of membrane potential from V_H of −60 mV. (○) Current in Na^+, K^+-free $Tris^+$, Cs^+ Ringer and (●) current at 10 min after adding 3×10^{-5} M Verapamil.

The effect of divalent cations and La^{3+} upon Ca^{2+} current in the presence of Ca^{2+} can be determined using Hagiwara's modification of Eq. 1 (1975). Thus,

$$I_{Ca}(V) = \frac{I_{Ca\ max}(V)}{1 + [1 + [M^{2+}]_o/K_M(V)]K_{Ca}(V)/[Ca^{2+}]_o}. \quad (2)$$

The different K_M's were calculated using those concentrations that produced half inhibition of the transient Ca^{2+} current. The values are shown in Table II.

With respect to the calcium conductance, G_{Ca}, the results to this point indicate that I_{Ca} is concentration-dependent and that G_{Ca} contains a voltage-dependent site which binds divalent and trivalent cations. Changes in $[Ca^{2+}]_i$ appear to affect G_{Ca}, and changes in $[Ca^{2+}]_o$ which are also thought to affect the conductance-voltage relationship of I_{Ca} in snail neurons (Kostyuk et al., 1974*b*) were further analyzed using results obtained in zero Mg^{2+} solutions.

Effects of $[Ca^{2+}]_o$ upon G_{Ca}

G_{Ca} was calculated as a chord conductance using an E_{Ca} of 150 mV. As we shall see, this approach is reasonable at depolarizing voltages of 100–150 mV. In the

presence of Mg^{2+} the relationship between G_{Ca} and voltage (G_{Ca}-V) was little affected by halving or doubling $[Ca^{2+}]_o$ (Fig. 9 A). However, in the absence of Mg_o^{2+}, there were large effects over the entire voltage range (Fig. 9 B). At higher $[Ca^{2+}]_o$'s the S-shaped G_{Ca}-V curve was shifted to the right and vice versa at lower $[Ca^{2+}]_o$'s. Similar results have been reported for the G_{Ca}-V relationship in *Helix pomatia* neurons (Kostyuk et al., 1974*b*). Changes in the shape of the normalized G_{Ca}-V relationships were not apparent.

The above results were obtained assuming a chord conductance for G_{Ca}. However, as we have already noted, the inward current becomes small and usually disappears rather than reversing at large depolarizing voltages suggesting that current flow might be best predicted from constant field considerations. Therefore, the way in which voltage drives current through the Ca^{2+} conductance was examined further.

Instantaneous I-V Relationships of I_{Ca}

A sequence of two voltage steps was used. The first step elicited peak inward I_{Ca}, and at this time a second step to variable voltages was made. The instantaneous currents were derived by extrapolating the tail currents back to zero time for the second voltage step. The instantaneous I-V relationship so derived is linear up to 100–150 mV depending upon the particular neuron and is therefore described by a chord conductance over most of its range (Fig. 9 C). The chord conductance had a value of $0.16 \pm 0.02 \times 10^{-6}\ \Omega^{-1}$ (four cells). At

TABLE II

DISSOCIATION CONSTANTS FOR VARIOUS Ca^{2+} ANTAGONISTS

Ca^{2+} antagonist	Half inhibition dose	K_M
Ni^{2+}	0.03	0.15
La^{3+}	0.23	1.15
Cd^{2+}	2.2	11.0
Co^{2+}	4.18	20.9

K_M values were calculated from Eq. 2 using K_{Ca} = 5.4 mM.

FIGURE 9 (*Opposite*). Conductance-voltage relationships of I_{Ca}. (A) Conductance relative to maximum conductance obtainable in a neuron soaked in Na^+, K^+-free $Tris^+$, Cs^+ Ringer solution containing 15 mM Mg^{2+} is plotted against the membrane potential. V_H: −60 mV. Symbols △, ○, and ● indicate 2, 10, and 40 mM $[Ca^{2+}]_o$ test solutions, respectively. Conductance was calculated as a chord conductance assuming E_{Ca} of 150 mV. (B) Ca^{2+} conductance as function of membrane potential of a neuron in Na^+, K^+, Mg^{2+}-free $Tris^+$, Cs^+ Ringer solution. V_H: −70 mV. Symbols ■, ○, and ● indicate the measurements in 2, 10, and 40 mM $[Ca^{2+}]_o$ test solutions. (C) Instantaneous I-V relationships in two different neurons determined from a sequence of two voltage steps. The second voltage step of variable amplitude was applied when the Ca^{2+} inward current produced by a voltage step to +15 mV was maximal. The current produced by the second step was extrapolated back to zero time for the second step. V_H: −60 mV. Note that the I-V relationships are linear over a large range, but at very high voltages I_{Ca} appears to curve away from the voltage axis.

very high voltages I_{Ca} appears to bend away from the voltage axis. There is some uncertainty about this region, however, because an average leakage correction term which is relatively large had to be used (see Fig. 8, Lee et al.).

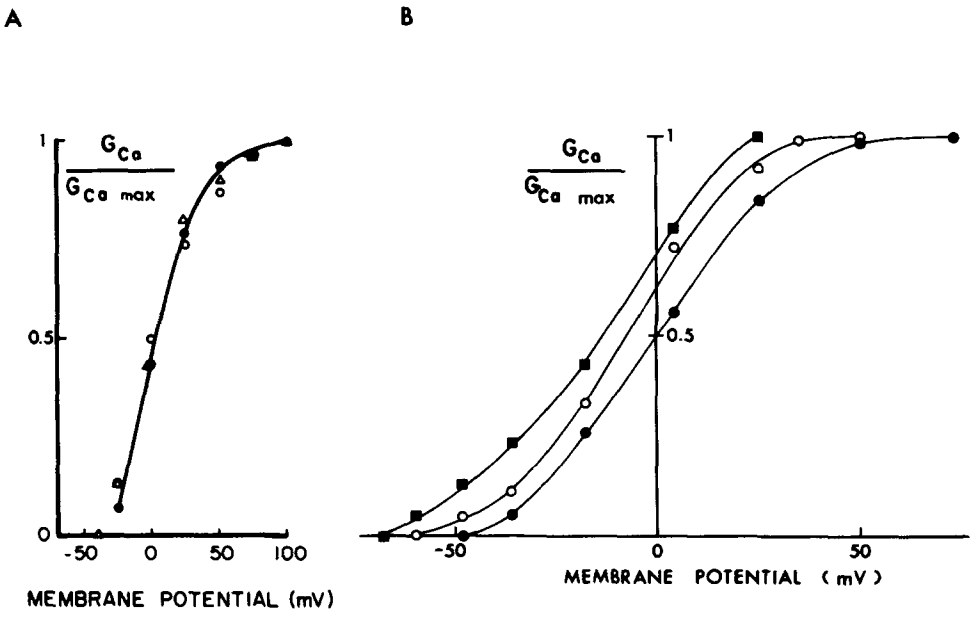

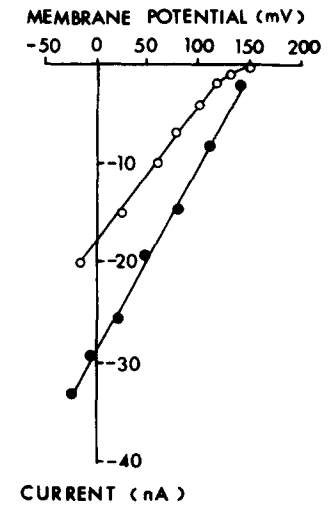

An attempt was made to fit the entire *I-V* relationship using a calcium permeability calculated following Fatt and Ginsborg (1958) as

$$P_{Ca} = I_{Ca}\, RT/4F^2V\, [\exp 2\, VF/RT - 1/Ca_i\, (\exp 2\, VF/RT) - Ca_o]. \quad (3)$$

Fits could only be obtained when P_{Ca} was allowed to vary from values of $\cong 10^{-8}$

$-10^{-9} \cdot cm^3 \cdot s^{-1}$ over the voltages shown in Fig. 9C, the higher values of P_{Ca} corresponding to the smaller voltages. It seems reasonable therefore to treat the instantaneous *I-V* relationship as a chord conductance.

Inactivation of I_{Ca}

h_∞, the Hodgkin-Huxley steady-state inactivation parameter (1952*a*) was examined using conditioning pulses 30–200 ms in duration and a test pulse that evoked peak inward I_{Ca}. The ratio of $I_{Ca(0)}$, the peak current elicited without a prepulse and I_{Ca} (V), the peak current elicited with a prepulse preceding the test step were used as the measure of h_∞. There was no inactivation at the holding potential of −60 mV (Fig. 10 A) and an S-shaped h_∞-V curve at test voltages of +15 mV is fitted by

$$h_\infty = 1/(1 + \exp[(V - V_H)/12 \text{ mV}]), \quad (4)$$

where V_H is −16 mV, the value at which $h_\infty = 0.5$.

The h_∞-V relationship was influenced by the magnitude of the test voltage step. At larger test steps the curve was shifted to the right (Fig. 10 B). Similar results have been reported in *Myxicola* and squid axons (Goldman and Schauf, 1973; Goldman, 1976) and are predicted when inactivation and activation are coupled rather than independent as in Hodgkin-Huxley theory. Further evidence for activation-inactivation coupling came from studies of inactivation time constants. The time constant of inactivation as a function of voltage τ_h was calculated from the fall in Ca^{2+} transient current at different voltages. It was also calculated as τ_c (Fig. 11 B), using prepulses of varying duration and voltage and a constant test voltage that elicited the peak transient Ca^{2+} current inasmuch as the reduction in the test current with increasing prepulse duration was fitted after a slight delay by a single exponential function (Fig. 12 A). The voltage dependence of τ_h and τ_c are compared in Fig. 11 B. τ_h is smaller than τ_c and such differences are also predicted if there is coupling between activation and inactivation (Goldman, 1976).

The same experiments allowed us to examine the possibility that inactivation was delayed in its onset, a result also consistent with an activated state preceding inactivation. The results are shown in Fig. 12. I_{Ca}'s elicited by test steps were unaffected by prepulses <0.8 ms in duration indicating a delayed onset of inactivation.

In none of our experiments have we ever observed facilitation of I_{Ca} by prepulses as reported by Eckert et al. (1977) (Fig. 11 A).

Activation of I_{Ca}

The onset of I_{Ca} is difficult to determine because the capacitative current transient may persist for 500 μs. At longer times I_{Ca} has a rising phase that can be fitted by a monoexponential function. G_{Ca} can be decomposed into two components and may be described by

$$G_{Ca} = \bar{G}_{Ca}\, m\, h, \quad (5)$$

where m, h, and $\bar{G}_{Ca}$ are used according to Hodgkin-Huxley symbolism (1952 b). An m^2h function gave an equally good fit while providing a small delay to the

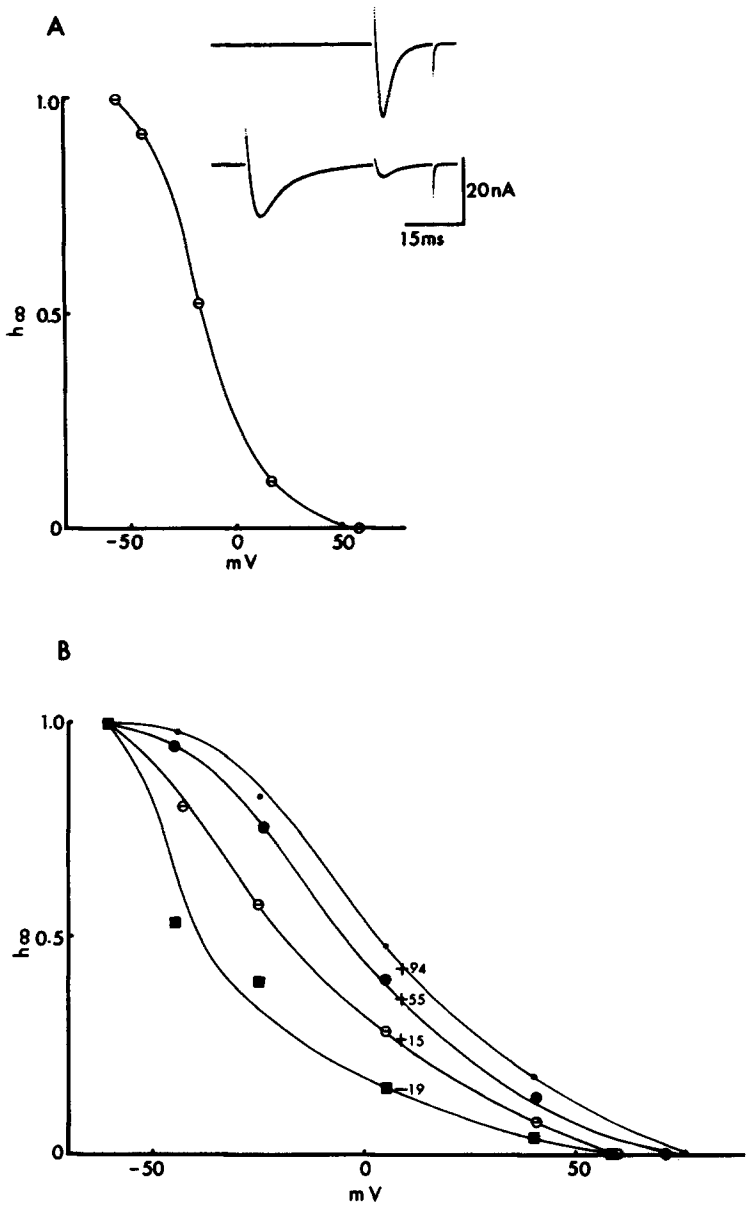

FIGURE 10. Steady-state relation for inactivation of $I_{Ca^{2+}}$. (A) V_H: −60 mV. Test pulse is a voltage step to +15 mV, 20 ms in duration. Ordinate: h_∞ plotted as the ratio of I_o to I_V (see text for definitions). Abscissa: the voltage step of prepulse 30 ms in duration. The continuous curve is drawn according to Eq. 4. The inset shows the currents elicited by the test step with and without a prestep. (B) Effects of different values of test pulse on the relation between h_∞ and membrane potential. V_H: −60 mV. The different voltage steps of test pulses 30 ms in duration are shown for each curve. Ordinate: h_∞. Abscissa: the voltage step of prepulse. The curves for −19, +15, +55, and +94 mV were fitted by eye.

onset of I_{Ca}. It was simpler to use m to the first power, and steady-state activation, m_∞, was calculated directly as the ratio of chord conductance to peak chord conductance and its relationship to voltage is shown in Fig. 13 A.

τ_m was calculated in two ways: (*a*) by measuring the time constant required to attain peak I_{Ca} after correcting for inactivated current or (*b*) by measuring the time constant of the current tails when the voltage was stepped to new values at

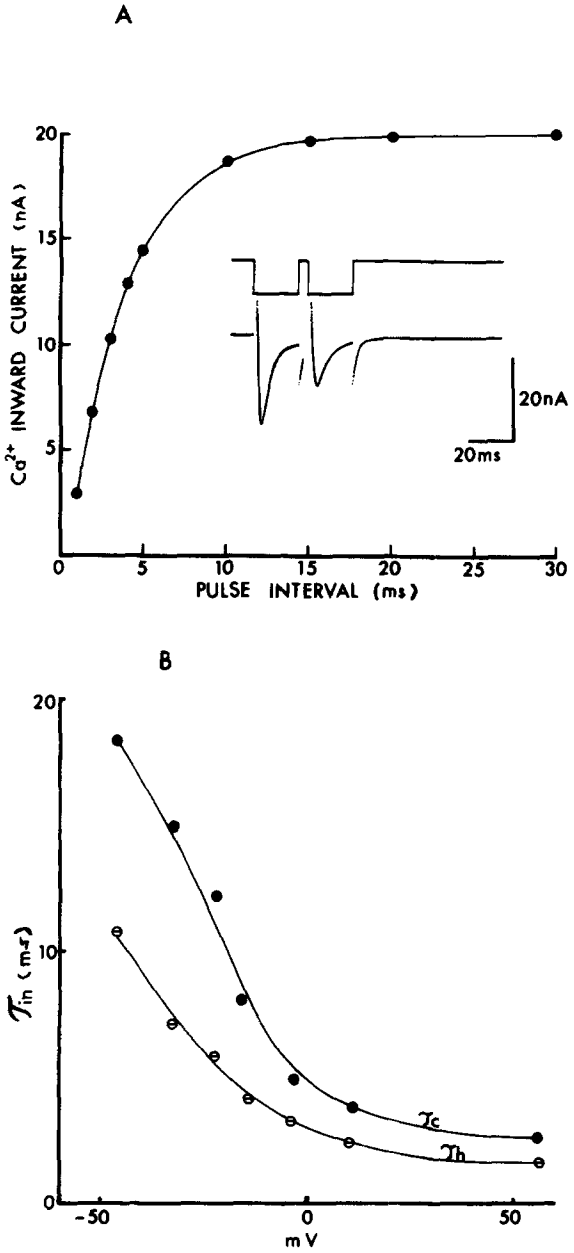

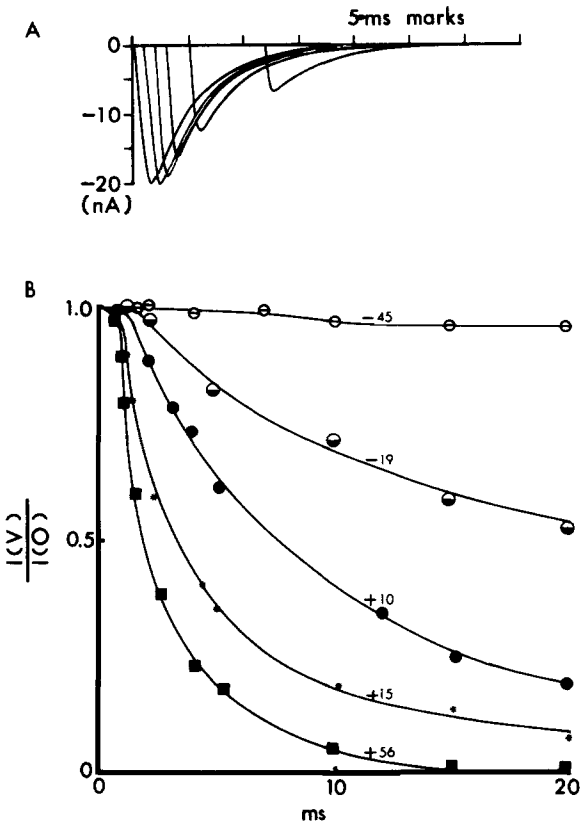

FIGURE 12. Onset of inactivation using the prestep plan described for Fig. 11. (A) Currents elicited by the test pulse at variable times after the prestep was initiated. Test pulse: voltage step, +15 mV and 20 ms in duration. Test pulse currents at prepulses <0.8 ms in duration are unaffected by the prepulse. (B) Delayed onset of inactivation at different prestep amplitudes. Ordinate: $I(V)$ and $I(0)$ indicate ratio of peak Ca^{2+} inward currents with and without prepulses. Abscissa: the prepulse duration. The values beside each curve indicate the prestep amplitude. Note the delayed onset of Ca^{2+} current inactivation when the prepulse duration was <0.8–1.0 ms.

FIGURE 11 (*Opposite*). (A) Absence of facilitation of I_{Ca} and (B) evidence for coupling of activation and inactivation in snail neurons. (A) Plot of the current amplitude evoked by the second of two equivalent voltage steps with variable intervals between the steps. At intervals <20 ms the current evoked by the second step is reduced, and at longer intervals there is recovery. However, no facilitation is observed. The recovery is exponential. Varying the amplitude and duration of the prepulses allow τ_c to be evaluated as in B. (B) Comparison of current, τ_c, with the time constant of inactivation, τ_h, determined from test pulses of variable amplitude and 20 ms in duration. The test pulse used with the prepulses was +15 mV and 20 ms in duration. V_H: −60 mV. Ordinate: $\tau_{\text{inactivation}}$. Abscissa: the voltage steps of test pulses 20 ms in duration. Symbols ● and ⊖ show the measurements of τ_c and τ_h.

the time of peak I_{Ca}. The τ_m-voltage relationships appeared similar using either method (Fig. 13 B).

DISCUSSION

The Ca^{2+} conductance we have identified does not transport Na^+. This agrees with the recent conclusions of Kostyuk et al. (1977) and differs from earlier reports from the same laboratory (Kostyuk et al., 1974*a*, *b*). The null potential for I_{Ca} is very positive and is consistent with the measured Ca^{2+} activity gradients. The lower reversal potentials reported by Kostyuk et al. (1974*a*) and Standen (1975) may be due to the presence of K^+ current in their experiments.

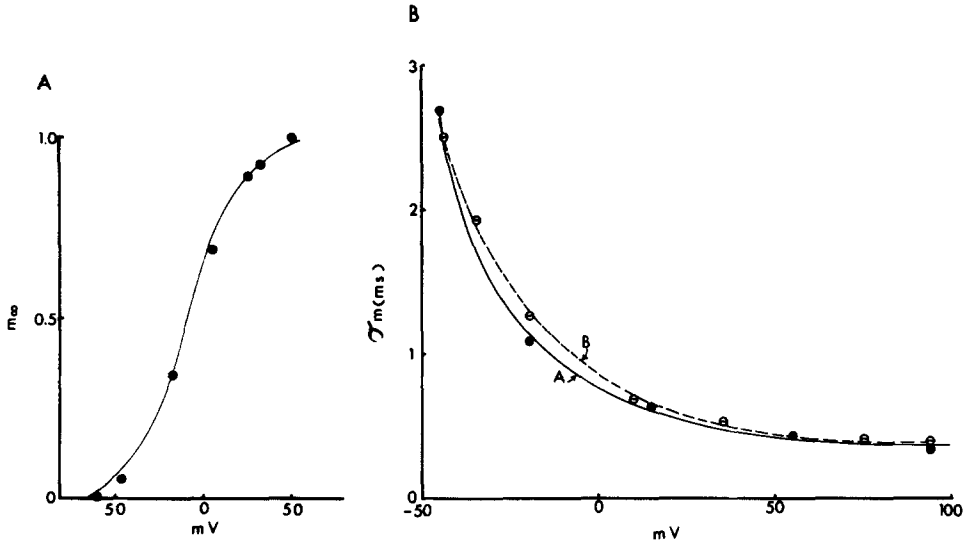

FIGURE 13. Activation parameters for I_{Ca}. (A) m_∞-voltage curve with $m_\infty = G_{Ca}/G_{Ca}$. (B) Comparison of τ_m-voltage relationships where curve A gives the values for time constant to peak current and curve B gives the values for time constants of tail currents elicited by a second voltage step delivered at the time of the peak inward current. The differences were not consistent from cell to cell and were within the range of error of the measurement.

This may also account for the clear-cut reversal potentials of their peak current vs. voltage (*I-V*) curves inasmuch as we have found that when the Na^+ and K^+ currents are suppressed reversal currents are obscured by leakage currents and clear reversal potentials are the exception, not the rule. In fact, those cells showing reversal potentials had lower membrane resistances and did not survive as well, which may be attributable to elevated $[Ca^{2+}]_i$ levels at the membrane. At voltages <100–150 mV, the instantaneous *I-V* curve is linear and a chord conductance was used for modelling purposes and to calculate conductance-voltage relationships from peak current vs. voltage curves. The shape of the instantaneous *I-V* curve was uncertain at very high voltages and led to a consideration of a permeability term using constant field theory. However, a good fit could only be obtained when the permeability coefficient was allowed to vary 10-fold over the voltage range examined so this model was excluded.

The conductance-voltage relationship was shifted by $[Ca^{2+}]_o$ when $[Mg^{2+}]_o$ was zero, and these observations support the reports of Kostyuk et al. (1974*a*, *b*) and Standen (1975) and are similar to the effects of Ca^{2+} on the relationship between G_{Na} and voltage observed in squid axon (Frankenhaeuser and Hodgkin, 1957). Changes in $[Ca^{2+}]_i$ had opposite effects on the conductance-voltage relationship and both effects may be due to a similar action of Ca^{2+} on membrane surface charge (McLaughlin et al., 1971).

The Ca^{2+} conductance in its voltage and time dependence has some similarities to the Na^+ conductances of axons. Some important differences, however, are that the Ca^{2+} conductance saturates at modest elevations of $[Ca^{2+}]_o$'s, conducts at least two ions, Ba^{2+} and Sr^{2+}, better than Ca^{2+} and is blocked by small doses of other divalent cations such as Ni^{2+}, Cd^{2+}, and Co^{2+} and the trivalent cation La^{3+}. The most satisfactory explanation of these results is the binding model proposed for barnacle muscle by Hagiwara (1975). Thus, the conductance contains a site which binds Ca^{2+} more strongly than Ba^{2+} or Sr^{2+}. According to Hagiwara (1975), when Co^{2+} is bound to the site, the Ca^{2+} conductance transfers Ca^{2+} better than Ba^{2+} or Sr^{2+}; but in our experiments these three ions were transported equally well in the presence of Co^{2+}. However, the conductance of Ca^{2+} relative to Ba^{2+} and Sr^{2+} was less inhibited by Co^{2+} (cf. A and B of Fig. 6). The binding site also appears to be voltage-dependent which is a new finding and suggests that it is within the membrane voltage field.

Increases in $[Ca^{2+}]_i$ in addition to shifting the null potential of I_{Ca} according to a Nernst-type relation, appear to suppress peak I_{Ca} to an even greater extent. This suppression cannot be accounted for by the same equation that accounts for the actions of changes in $[Ca^{2+}]_o$ on I_{Ca} so that $[Ca^{2+}]_i$ changes probably do not act at the more external Ca^{2+} binding site.

Kinetics of I_{Ca}

The conductance kinetics using the Hodgkin-Huxley scheme are described by m and h parameters with m to the first rather than to the more usual higher powers. However, the earliest component of I_{Ca} has not been resolved and a small delay may be present. m to the second power describes the present data just as well as m to the first power and has been used by Kostyuk et al. (1977). Because it was simpler we used m to the first power in our calculations. Using values for h_∞, m_∞, τ_m, and τ_h given in Table III, the forward and backward rate constants α_m, β_m, α_h, and β_h as functions of voltage may be determined (Fig. 14). Theoretical I_{Ca}'s are represented by G_{Ca}'s assuming chord conductances and adequately reflect the experimental results given that the parameters were derived from the average values obtained from different cells (Fig. 15). The slowly inactivating component which is so apparent at small depolarizations is accounted for by negligible values for β_h at these voltages (Fig. 14).

However, we have found substantial evidence that activation and inactivation of the Ca^{2+} conductance are coupled and a simple kinetic model for coupling also gives results that fit the experimental data (Fig. 15). In this model,

$$x \underset{\beta_m}{\overset{\alpha_m}{\longleftrightarrow}} y \underset{l}{\overset{k}{\longleftrightarrow}} z,$$

where x is the resting state, y, the activated state, z the inactivated state, α_m and β_m are the Hodgkin-Huxley parameters and k and l the forward and backward rate constants for the inactivating step. Slightly more complicated models of a

TABLE III
AVERAGE VALUES FOR I_{Ca} HODGKIN-HUXLEY PARAMETERS IN SNAIL NEURONS

Voltage	m_∞*	τ_m	h_∞‡	τ_h
mV		*ms*		*ms*
−45	0.06	2.70	1.00	10.00
−19	0.34	1.01	0.54	8.00
+15	0.80	0.70	0.11	5.30
+94	1.00	0.35	0.00	1.80

* m_∞ and τ_m values were averaged from four cells.
‡ h_∞ and τ_h values were averaged from a different set of four cells.

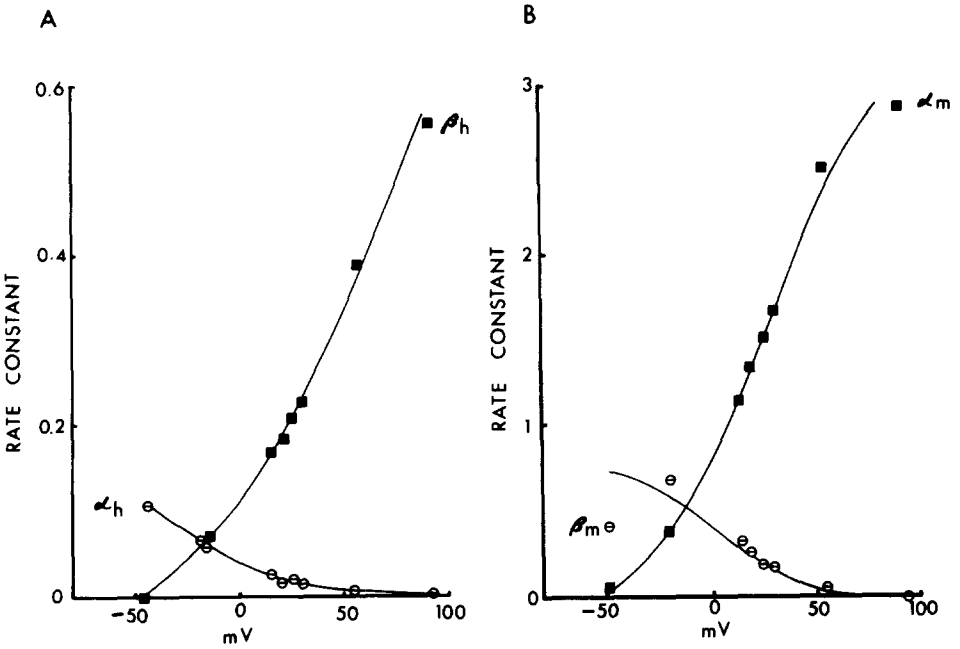

FIGURE 14. Rate constants for (A) inactivation process and (B) activation process calculated using the Hodgkin-Huxley model. Values were obtained from $\tau_m(V) = 1/(\alpha_m + \beta_m)$ and $m_\infty(V) = \alpha_m(V)/(\alpha_m[V] + \beta_m[V])$. Similar expressions were used for solving α_h and β_h.

similar nature have been used for K^+ channels (Armstrong, 1966, 1971) and for Na^+ channels by Moore and Jakobsson (1971); the particular model we used was first suggested to us by Dr. C. Armstrong. At rest all of the channels are in state x. After depolarization the reaction moves to the right and most of them end in state z. The reactions are represented by three linear first order differential equations and were determined analytically by taking the Laplace transform of

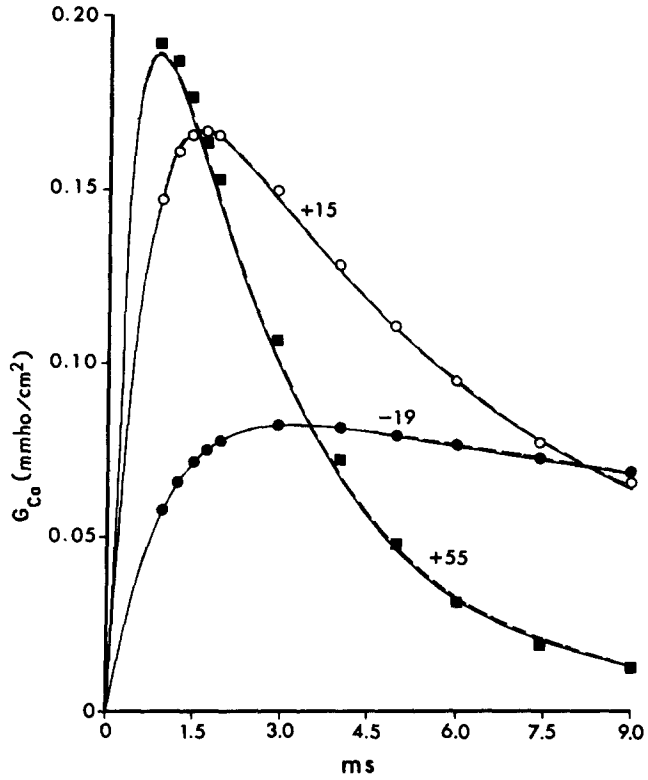

FIGURE 15. Comparison of experimental data (symbols) from one neuron with the values predicted by the Hodgkin-Huxley model (solid line) and the coupled model (dashed line). Both models fit the data equally well and the fits remain relatively good out to times of 100 and 1,000 ms. The equation for the coupled model is given in the text (Eq. 6) and the equation for Hodgkin-Huxley model was Eq. 5, and $m = m_\infty(1 - \exp -t/\tau_m)$ and $h = h_\infty - (h_\infty - 1)\exp^{-t/\tau_h}$, where $m_0 = 0$ and $h_0 = 1$ at $V_H = -60$ mV.

each, solving the third order determinant, and taking the inverse transform. Each solution is the sum of two exponentials. For example,

$$y(\tau) = \alpha_m/(a - b)[(l/a - 1)e^{-a\tau} + (-l/b + 1)l^{-b\tau}] + \alpha_m l/ab, \quad (6)$$

where

$$a + b = k + l + \alpha_m + \beta_m, \quad (7)$$

and

$$a \cdot b = \alpha_m k + \alpha_m l + \beta_m l. \quad (8)$$

The values for k and l used to fit the data were obtained by trial and error fits to the analytical solutions of the rate equations and are given in Table IV. At low depolarizations the rate constants are small, and with β_m large enough, many of the channels are in state x forming a reservoir which keeps y at a steady level for long times. If the relative value of rate constant l is large enough, y

persists almost indefinitely and the slowly inactivating component of I_{Ca} is observed. As we have already shown, this also occurs when an appropriate choice of rate constants is made using the uncoupled Hodgkin-Huxley model. Thus, I_{Ca} has an activation component and a single inactivation component for times up to 50 ms, and it does not seem necessary to postulate a distinct conductance for the persistent inward current as has been suggested (Eckert and Lux, 1976; Magura, 1977). It also appears that either model, coupled or noncoupled, can fit the voltage clamp currents so that small latencies in the onset of inactivation do not alter the currents detectably.

TABLE IV

RATE CONSTANTS USED FOR COUPLED MODEL OF I_{Ca}

Voltage	α_m	β_m	k	l
mV			ms^{-1}	
−45	0.02	0.35	0.000001	0
−19	0.34	0.65	0.15	0.05
+15	1.15	0.42	0.23	0.024
+94	3.0	0.12	0.65	0.000001

We thank Dr. R. Horn and Dr. L. E. Moore for reading the manuscript and for helpful suggestions. This work was supported by grant NS-11453 from the U.S. Department of Health, Education, and Welfare.

Received for publication 7 September 1977.

REFERENCES

ARMSTRONG, C. M. 1966. Time course of TEA^+-induced anomalous rectification in squid giant axons. *J. Gen. Physiol.* **50**:491–503.

ARMSTRONG, C. M. 1971. Interaction of tetraethylammonium ion derivatives with the potassium channels of giant axons. *J. Gen. Physiol.* **58**:413–437.

BAKER, P. F., A. L. HODGKIN, and E. B. RIDGWAY. 1971. Depolarization and calcium entry in squid giant axons. *J. Physiol. (Lond.)* **218**:709.

ECKERT, R., and H. D. LUX. 1976. A voltage-sensitive persistent calcium conductance in neuronal somata of *Helix*. *J. Physiol. (Lond.)*. **254**:129.

ECKERT, R., D. TILLOTSON, and E. B. RIDGWAY. 1977. Voltage-dependent facilitation of Ca^{2+} entry in voltage-clamped, aequorin-injected molluscan neurons. *Proc. Natl. Acad. Sci. U. S. A.* **74**:1748.

FATT, P., and B. L. GINSBORG. 1958. The ionic requirements for the production of action potentials in crustacean muscle fibres. *J. Physiol. (Lond.)*. **142**:516.

FATT, P., and B. KATZ. 1953. The electrical properties of crustacean muscle fibres. *J. Physiol. (Lond.)*. **120**:171.

FRANKENHAEUSER, B., and A. L. HODGKIN. 1957. The action of calcium on the electrical properties of squid axons. *J. Physiol. (Lond.)*. **137**:218.

GOLDMAN, L. 1976. Kinetics of channel gating in excitable membranes. *Q. Rev. Biophys.* **9**:491.

GOLDMAN, L., and C. L. SCHAUF. 1973. Quantitative description of sodium and potassium currents and computed action potentials in myxicola giant axons. *J. Gen. Physiol.* **61**:361–384.

HAGIWARA, S. 1975. Ca-dependent action potential. *In* Membranes. G. Eisenman, editor. Marcel Dekker, Inc., New York. 359–382.

HAGIWARA, S., and K-I. NAKA. 1964. The initiation of spike potential in barnacle muscle fibers under low intracellular Ca^{++}. *J. Gen. Physiol.* **48**:141–162.

HAGIWARA, S., and K. TAKAHASHI. 1967. Surface density of calcium ions and calcium spikes in the barnacle muscle fiber membrane. *J. Gen. Physiol.* **50**:583–601.

HENCEK, M., and J. ZACHAR. 1977. Calcium currents and conductances in the muscle membrane of the crayfish. *J. Physiol. (Lond.).* **268**:51.

HODGKIN, A. L., and A. F. HUXLEY. 1952*a*. The dual effect of membrane potential on sodium conductance in the giant axon of *Loligo*. *J. Physiol. (Lond.).* **116**:497.

HODGKIN, A. L., and A. F. HUXLEY. 1952*b*. A quantitative description of membrane current and its application to conduction and excitation in nerve. *J. Physiol. (Lond.)* **117**:500.

KATZ, B., and R. MILEDI. 1967. A study of synaptic transmission in the absence of nerve impulses. *J. Physiol. (Lond.).* **192**:407.

KOSTYUK, P. G., O. A. KRISHTAL, and P. A. DOROSHENKO. 1974*a*. Calcium currents in snail neurones. I. Identification of calcium current. *Pfluegers Arch. Eur. J. Physiol.* **348**:83.

KOSTYUK, P. G., O. A. KRISHTAL, and P. A. DOROSHENKO. 1974*b*. Calcium currents in snail neurones. II. The effect of external calcium concentration on the calcium inward current. *Pfluegers Arch. Eur. J. Physiol.* **348**:95.

KOSTYUK, P. G., O. A. KRISHTAL, and Y. A. SHAKHOVALOV. 1977. Separation of sodium and calcium currents in the somatic membrane of mollusc neurons. *J. Physiol. (Lond.).* **270**:545.

LEE, K. S., N. AKAIKE, and A. M. BROWN. 1977. Properties of internally perfused, voltage-clamped, isolated nerve cell bodies. *J. Gen. Physiol.* **71**:489–507.

MAGURA, I. S. 1977. Long-lasting inward current in snail neurons in barium solutions in voltage-clamp conditions. *J. Membr. Biol.* **35**:239.

MARTELL, A. E., and L. G. SILLÉN. 1971. Organic ligands including macromolecular ligands. *In* Stability Constants of Metal Ion Complexes. Chemical Society (London), Publishers. 76, 90.

MCLAUGHLIN, S. G., G. SZABO, and G. EISENMAN. 1971. Divalent ions and the surface potential of charged phospholipid membranes. *J. Gen. Physiol.* **58**:667–687.

MOORE, L. E., and E. JAKOBSSON. 1971. Interpretation of the sodium permeability changes of myelinated nerve in terms of linear relaxation theory. *J. Theor. Biol.* **33**:77.

STANDEN, N. B. 1975. Voltage clamp studies of the calcium inward current in an identified snail neurone: comparison with the sodium inward current. *J. Physiol. (Lond.).* **249**:253–268.